Biochimica et Biophysica Acta, 459 (1977) 119–137
© Elsevier/North-Holland Biomedical Press

BBA 47227

BINDING OF HQNO TO BEEF-HEART SUB-MITOCHONDRIAL PARTICLES

GERRIT VAN ARK and JAN A. BERDEN

Laboratory of Biochemistry, B.C.P. Jansen Institute, University of Amsterdam, Plantage Muidergracht 12, Amsterdam (The Netherlands)

(Received May 28th, 1976)

SUMMARY

1. The fluorescence spectra of HQNO (2-*n*-heptyl-4-hydroxyquinoline-*N*-oxide) in water at pH 7.5 show an emission maximum at 480 nm and an excitation maximum at 355 nm.

2. The fluorescence is enhanced by binding to bovine serum albumin, and is completely quenched by binding to sub-mitochondrial particles of beef heart.

3. Binding experiments reveal specific binding of HQNO to sub-mitochondrial particles with a dissociation constant of 64 nM and, depending on the protein concentration, a considerable amount of aspecific binding.

4. The concentration of specific binding sites for HQNO is identical with that of antimycin-binding sites. Furthermore, the presence of antimycin prevents the binding of HQNO and antimycin releases HQNO from its binding site.

5. The binding of HQNO is not sensitive to the redox state of the respiratory-chain components.

6. Inhibition of electron transfer by HQNO is caused by binding to the specific binding site.

7. The relation between inhibition of NADH or succinate oxidation and saturation of the binding site is hyperbolic.

8. The increase in the reduction level of cytochrome *b* on addition of HQNO in the presence of succinate and oxygen, either in the presence or absence of cyanide, does not parallel the inhibition of overall electron transfer.

9. All data can be quantitatively described and analysed using the model for electron transfer proposed by Wikström and Berden in 1972 (Wikström, M. K. F. and Berden, J. A. (1972) Biochim. Biophys. Acta 283, 403–420).

INTRODUCTION

Antimycin has proved a useful tool in the study of the electron pathway through the ubiquinol-ferricytochrome *c* oxidoreductase segment (Complex III) of the respiratory chain. It has the advantage that the binding is so strong that until

Abbreviation: HQNO, 2-*n*-heptyl-4-hydroxyquinoline-*N*-oxide.

nearly full saturation has been reached the amount of antimycin bound virtually equals the amount added, the amount of free antimycin being negligible. On the other hand, this strong binding has caused difficulties in the interpretation of the sigmoidal curves relating the inhibition of substrate oxidation and the increased reduction of cytochrome *b* in the presence of cyanide (and oxygen) to the concentration of added antimycin.

Bryła et al. [1, 2] proposed in 1969 that antimycin is an allosteric inhibitor that stabilizes an inhibited conformation of the QH_2-cytochrome *c* oxidoreductase, in which the reduction of cytochrome *b* is promoted. The sigmoidicity of the effect curves was explained by multiple interacting antimycin-binding sites. This proposal obtained support from the experiments of Berden and Slater [3] which showed that, in the presence of substrate but not in its absence, the binding of antimycin is positive cooperative.

Kröger and Klingenberg, however, have pointed out that, in view of the well-documented pool function of ubiquinone [4], a hyperbolic inhibition curve may be expected if the antimycin-sensitive part of the respiratory chain (oxidation of ubiquinol) has a larger intrinsic capacity for electron transfer than the antimycin-insensitive part (reduction of ubiquinone) [4–6]. According to these authors, and also Rieske and Das Gupta [7], the departure of the inhibition curve from a hyperbola at high antimycin concentrations, giving the appearance of sigmoidicity, is due to dissociation of the antimycin from its binding site at high saturation.

Although the model of Kröger and Klingenberg cannot explain the increased reduction of cytochrome *b* in the presence of cyanide and substrate, the refined kinetic model of Wikström and Berden [8] is able to do so, without invoking allostery [3, 9] or requiring a change in the midpoint potential of cytochrome *b* [10–12]. However, the only quantitative analysis of the experimentally determined antimycin-effect curve for the increased reduction of cytochrome *b* has been made on the basis of the allosteric model [3].

In an attempt to resolve these differences, a comparative study has been made of the effects of antimycin with those of a similar inhibitor of the QH_2-cytochrome *c* oxidoreductase segment of the respiratory chain, namely the chemically related 2-*n*-heptyl-4-hydroxyquinoline-*N*-oxide (HQNO) [13–15] which has similar effects [16, 17] and is believed, on kinetic grounds, to act at the same site [18]. In this paper we describe some results from which it is clear that HQNO indeed binds to the same site as antimycin but, unlike the latter, it has no allosteric properties. The results have been analysed quantitatively using the model for electron transfer proposed by Wikström and Berden [8] and Berden [19]. The differences between antimycin and HQNO will be analysed in a forthcoming paper.

Some of the results have been reported before [20, 21].

EXPERIMENTAL

Sub-mitochondrial particles were prepared from heavy beef-heart mitochondria according to Fessenden and Racker [22] (A particles) or Lee and Ernster [23] (EDTA particles).

If not stated otherwise the reaction mixture contained 250 mM sucrose, 10 mM $MgCl_2$, 1 mM EDTA and 50 mM Tris · HCl buffer at pH 7.5 (standard medium).

Fluorescence spectra were measured with a Perkin-Elmer spectrofluorimeter (MPF-2A), other fluorescence measurements were carried out in an Eppendorf photometer (1101 M) with fluorescence attachment, primary filter 313+366 nm, secondary filter 420–3000 nm. These filters are suitable for measuring the fluorescence of both antimycin and HQNO. The cell compartments were kept at 23 °C with a thermostat.

Respiratory activities were measured at 25 °C in an Oxygraph supplied with a Y.S.I. 5331 electrode. Inhibition of the NADH oxidase of sub-mitochondrial particles by HQNO and/or antimycin was measured by suspending the particles in the standard medium to which were added 3 μM horse-heart cytochrome *c* and the inhibitor(s). After 2 min, respiration was started by the addition of 0.6 mM NADH. Inhibition of the succinate oxidase of sub-mitochondrial particles by HQNO was measured by suspending the particles in the standard medium to which 20 mM succinate, 8 μM horse-heart cytochrome *c* and HQNO were added. After 5 min, oxygen uptake was measured by transferring the mixture to the Oxygraph vessel and adding 3 vols. of standard medium supplemented with 20 mM succinate.

Cytochrome *b* reduction was measured with an Aminco-Chance double-beam spectrophotometer (DW 2). The cuvette holder was thermostatted at 25 °C. Absorbance measurements in clear solutions were made with a Cary-17 spectrophotometer.

Antimycin and HQNO were added in ethanolic solutions in such a concentration that the ethanol concentration did not exceed 1 % (v/v). Antimycin was obtained from the Nutritional Biochemical Corporation. Its concentration was determined spectrophotometrically in ethanolic solution, using an absorbance coefficient at 320 nm of 4.8 $mM^{-1} \cdot cm^{-1}$ [24]. HQNO was obtained from Sigma. Its concentration was determined spectrophotometrically after dilution of an ethanolic stock solution in the standard medium, using an absorbance coefficient at 348 nm of 9.45 $mM^{-1} \cdot cm^{-1}$ [13] (see also Results). Protein was measured using the biuret reaction after precipitation of protein with trichloroacetic acid [25].

RESULTS

Measurement of HQNO

HQNO fluoresces with an emission maximum at 480 nm (Fig. 1A) and an excitation maximum at 355 nm (Fig. 1B), close to the absorbance maximum at 348 nm [13]. As is also the case with antimycin [3], the fluorescence of HQNO is enhanced (six-fold) upon binding to bovine serum albumin (Fig. 2A). The binding parameters can be derived from the titration of low concentrations of albumin (0.24 mg/ml) with HQNO (Fig. 2A). From these measurements the Scatchard plot [26] presented in Fig. 2B was constructed. One molecule of HQNO can be bound per molecule of albumin with a dissociation constant of 3.5 μM, which is 30-times higher than that of the albumin-antimycin complex ($K_D = 0.12$ μM [3]). We may conclude, then, that the fluorescence is not due to an impurity in the HQNO preparation, but is an intrinsic property of the molecule. Fluorescence determinations of HQNO in the presence of albumin are sensitive enough to allow accurate measurements of HQNO concentrations in the submicromolar range.

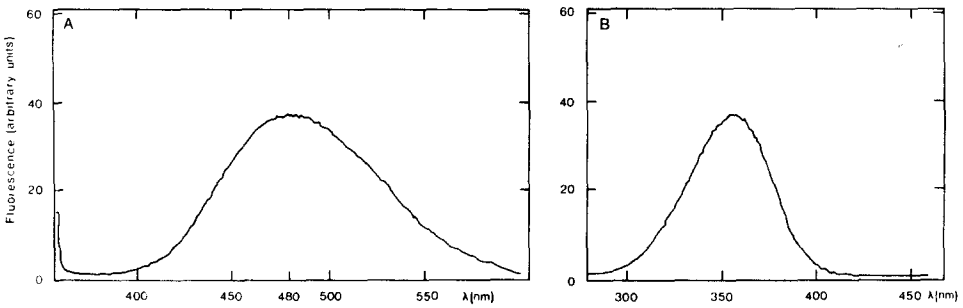

Fig. 1. Uncorrected fluorescence spectra of 23 μM HQNO dissolved in the standard medium. Excitation and emission slit widths were 4 nm. A. Emission spectrum (excitation at 355 nm). B. Excitation spectrum (emission at 480 nm).

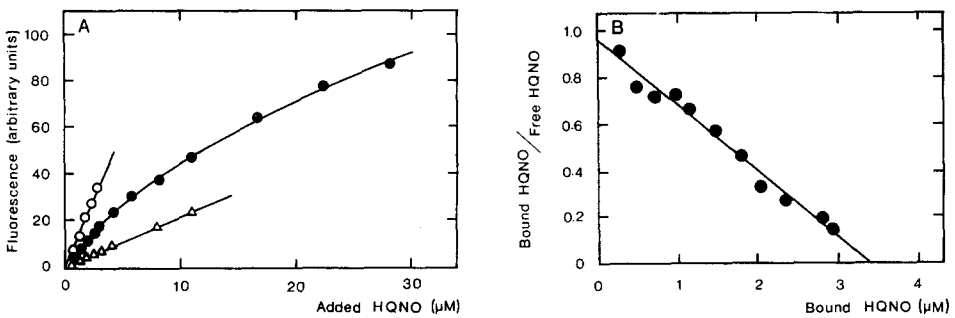

Fig. 2. Enhancement of HQNO fluorescence by binding to bovine serum albumin. A. A solution of 0.24 mg/ml albumin in standard medium was titrated with HQNO and the fluorescence measured after each addition (●—●). The fluorescence yield of bound HQNO was determined by titrating a high concentration (6 mg/ml) of albumin (○—○). The fluorescence yield of free HQNO was determined by titrating the standard medium in the absence of albumin (△—△). B. The experimental points of Fig. 2A were used to construct a Scatchard plot for the binding of HQNO to albumin. K_D = 3.5 μM, and the concentration of binding sites is 3.42 μM, i.e. 1 site per molecule of albumin (0.24 mg/ml = 3.55 μM).

Binding of HQNO to sub-mitochondrial particles

Binding of HQNO to sub-mitochondrial particles was determined by measuring the fluorescence in the supernatant after spinning down the particles from incubation mixtures containing different amounts of HQNO (Fig. 3A, +particles—antimycin). The reference is obtained by incubating the particles in the absence of HQNO, removing the particles by centrifugation and then titrating the supernatant with HQNO (Fig. 3A, —particles). The slope of the curve, +particles—antimycin, relating fluorescence with added HQNO becomes constant at higher HQNO concentrations, but is then only 45 % of that of the reference curve. This suggests that after the saturation of specific binding sites with HQNO, a considerable amount of HQNO can still be bound aspecifically. The occurrence of both specific and aspecific binding of HQNO is also shown when the HQNO-binding experiments are repeated, including in the incubation mixtures an amount of antimycin just enough to saturate the antimycin-binding sites (Fig. 3A, +particles+antimycin). The resulting linear titration

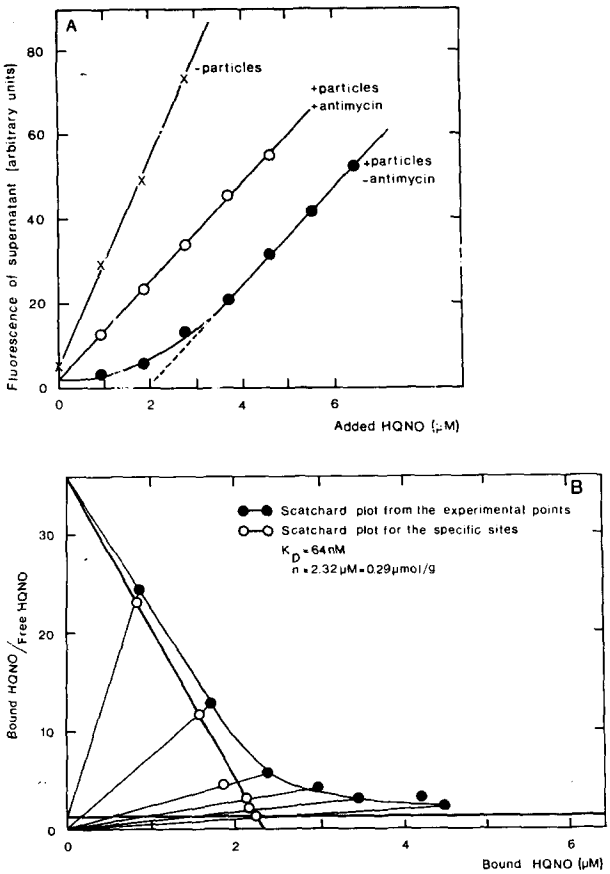

Fig. 3. Binding of HQNO to submitochondrial particles. A. A suspension of A particles (8.1 mg/ml) in standard medium was incubated with various amounts of HQNO for 10 min at 23 °C. After spinning down the particles for 10 min at 120 000 × *g*, the fluorescence of the supernatant was measured (● — ●). This experiment was repeated with 2.9 μM antimycin present in the incubation mixtures (○ — ○). For the reference the particles were incubated in the absence of HQNO, and after spinning down the particles the supernatant was titrated with HQNO (× — ×). B. ● — ●, Scatchard plot constructed from the experimental points of Fig. 3A, without correction for aspecific binding; ○ — ○, Scatchard plot corrected graphically for the contribution of the aspecific binding according to ref. 27. For this aspecific binding the ratio bound/free is 1.2 (from Fig. 3A, the experiment in the presence of antimycin). For the specific binding of HQNO K_D = 64 nM and n = 2.32 μM = 0.29 μmol/g protein.

curve has the same slope as that of the HQNO titration in the absence of antimycin at the higher concentrations of HQNO. It may be concluded that the saturation of the antimycin-binding sites prevents the subsequent binding of HQNO to the specific sites. The reverse experiment has also been done (not shown); after saturation of the specific binding sites with HQNO, the addition of antimycin gives rise to a fluorescence increase characteristic for HQNO. Apparently, antimycin, binding much stronger than HQNO, expells HQNO from the binding site. The experiment in the presence of antimycin thus allows separate estimation of the aspecific binding of HQNO. In the

present case about 55 % of the HQNO that is not bound to the specific sites is taken up by the membrane and 45 % remains in the water phase, or in other words, there is a partition coefficient (the ratio bound/free or the aspecific binding) of 1.2.

When the results of the experiment in the absence of antimycin are plotted in a Scatchard plot, using the reference experiment to calculate bound and free HQNO, the curve will be a summation of specific and aspecific binding (Fig. 3B). Since the contribution of the aspecific binding is known (the ratio bound/free is 1.2) a graphical correction [27] for this contribution can be made and the curve for the specific binding is obtained. From this plot a K_D of 64 nM is calculated. The concentration of HQNO-binding sites (0.29 μmol/g protein) is the same as the concentration of antimycin-binding sites (0.30 μmol/g protein) as determined in a parallel experiment (not shown).

Quenching of HQNO fluorescence upon binding to sub-mitochondrial particles

From a direct titration of a suspension of sub-mitochondrial particles, present in the fluorimeter cuvette (Fig. 4A), it can be seen that at low HQNO concentrations the fluorescence is quenched. It is possible to derive a Scatchard plot from such a titration (Fig. 4B) on the assumption that specifically bound HQNO is not fluorescent, whether or not the aspecifically bound HQNO fluoresces (see Appendix A). The same concentration of binding sites (0.28 μmol/g protein) as in the centrifugation experiments is calculated, but the apparent dissociation constant (140 nM) derived from this plot must be multiplied by a factor (0.45) equal to the fraction of free HQNO compared with the sum of free and aspecifically bound HQNO (see Appendix A). The real K_D is then 0.45×140 nM = 64 nM, in exact agreement with the value obtained in the centrifugation experiment.

Since the amount of aspecific binding (or the partition coefficient) is depen-

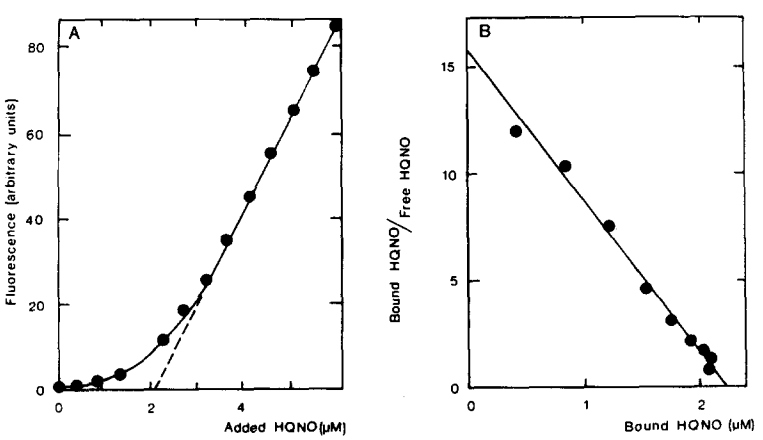

Fig. 4. Quenching of HQNO fluorescence by binding to sub-mitochondrial particles. A. A suspension of A particles (8.2 mg/ml) in standard medium was titrated with HQNO and the fluorescence measured after each addition. B. The experimental points of Fig. 4A were used to construct a Scatchard plot. It is assumed that bound HQNO is not fluorescent, and that the slope of the curve relating the fluorescence with added HQNO at higher HQNO concentrations represents the fluorescence of free HQNO. The apparent K_D = 140 nM and n = 2.25 μM = 0.28 μmol/g protein.

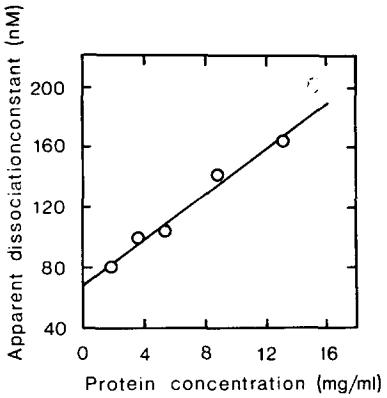

Fig. 5. The protein dependency of the apparent K_D. Suspensions of EDTA particles in standard medium with increasing protein concentration were titrated with HQNO and the K_D was calculated as described in Fig. 4. The intercept at the ordinate (69 nM) represents the real K_D of the particle · HQNO complex. The apparent K_D increases by 7.5 nM for each 1 mg/ml increase in protein concentration.

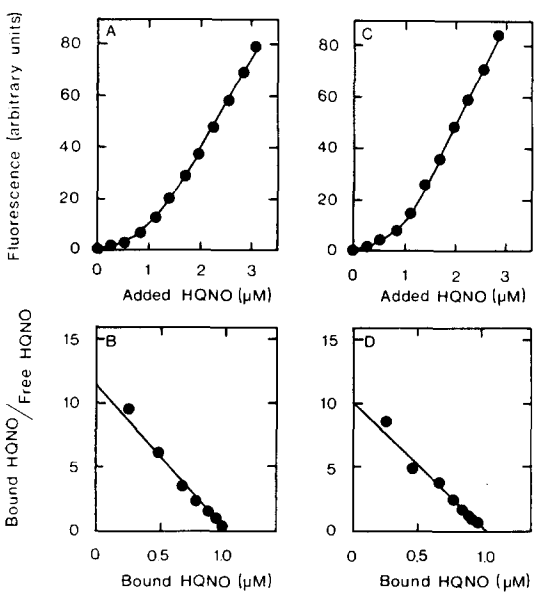

Fig. 6. The effect of reduction by succinate on binding of HQNO to sub-mitochondrial particles. Experimental conditions as in Fig. 4, with 3.1 mg/ml A particles. A. Without further additions (oxidized particles). B. Scatchard plot constructed from the experimental points of Fig. 6A. Apparent K_D = 90 nM and n = 1.03 μM = 0.33 μmol/g protein. C. 2 mM KCN+10 mM succinate added. D. Scatchard plot constructed from the experimental points of Fig. 6C. Apparent K_D = 105 nM and n = 1.06 μM = 0.34 μmol/g protein.

dent on the protein concentration, the apparent K_D determined from direct fluorimetric titrations is dependent on the protein concentration and the extrapolation to zero protein concentration also gives the real K_D (Fig. 5). From this graph a real K_D of 69 nM is determined. In experiments where it is necessary to know the amount of HQNO bound specifically at every concentration of added HQNO, it suffices to determine the apparent K_D under the conditions of the particular experiment from a single titration as shown in Fig. 4, since this gives the correct values for the HQNO bound specifically in this experiment (see Appendix A).

Since Berden and Slater [3] showed that the binding of antimycin to succinate-reduced particles is positive cooperative, in contrast to the non-cooperative binding to oxidized particles, the binding of HQNO to succinate-reduced particles was also measured. The binding of HQNO to both oxidized particles (Figs. 6A and B) and succinate-reduced particles (Figs. 6C and D) is non-cooperative. The apparent K_D, also nearly the same in both cases, is lower than the value found in the experiment of Fig. 4, owing to the lower protein concentration used in this experiment.

We conclude, therefore, that HQNO can not be considered as an allosteric ligand.

Inhibition of electron transfer by HQNO

Because it is now possible to measure the binding of HQNO to its specific site, it becomes possible to establish whether the inhibition of electron transfer by HQNO

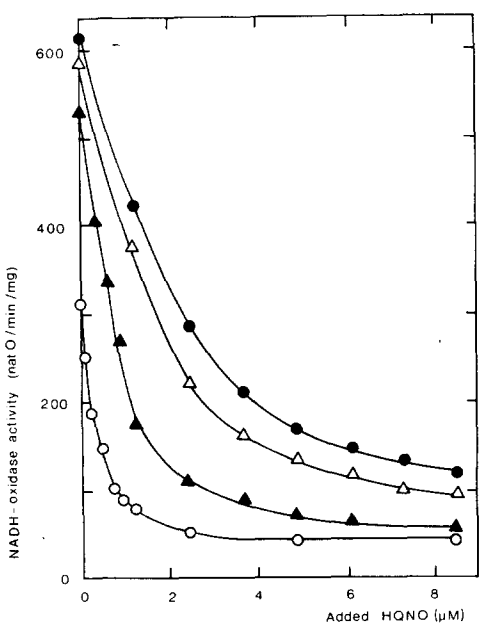

Fig. 7. Inhibition of NADH oxidase in sub-mitochondrial particles by HQNO. Oxygen uptake in the presence of various amounts of HQNO was measured as described in Experimental, with A particles (1.1 mg/ml). ●—●, no further additions, $c_{\frac{1}{2}} = 2.0\,\mu M$; △—△, 0.136 μmol/g antimycin present, $c_{\frac{1}{2}} = 1.5\,\mu M$; ▲—▲, 0.273 μmol/g antimycin present, $c_{\frac{1}{2}} = 0.8\,\mu M$; ○—○, 0.409 μmol/g antimycin present, $c_{\frac{1}{2}} = 0.3\,\mu M$. The total concentration of sites was 0.5 μmol/g protein.

is related to its binding to the specific site. Half-maximal inhibition of NADH oxidase occurs at 2 μM HQNO (Fig. 7). Since the apparent K_D at the protein concentration used (1.14 mg/ml) is about 80 nM, the inhibition does not seem to be related to the binding to the specific site. However, if it is assumed that the HQNO-sensitive step is not rate-limiting for the overall process of electron transfer from NADH to oxygen, this discrepancy is to be expected. To test this we added different amounts of antimycin to take away part of the excess capacity of the HQNO-sensitive step within the $b \cdot c_1$ complex. When the binding site is saturated with antimycin to the extent of 27, 52 and 82 %, the concentration of HQNO needed for half-maximal inhibition of the residual activity ($c_{\frac{1}{2}}$) declines to 1.5, 0.8 and 0.3 μM, respectively (Fig. 7). This is consistent with the postulate that the inhibition of the electron transfer by HQNO indeed occurs by binding to the specific binding site, and that the HQNO-sensitive step has a considerable excess capacity.

According to the model of Kröger and Klingenberg [4], the respiratory chain can be treated as two enzyme systems, one reducing Q (specific rate k_1) the other oxidizing QH_2 (specific rate k_2). The overall rate of electron transport then equals $k_1k_2/(k_1+k_2)$. If this is correct the form of the HQNO inhibition curves is determined by the ratio k_2/k_1, expressing the excess capacity of the HQNO-sensitive part of the respiratory chain over the dehydrogenase activity.

A comparison of the inhibitory effect of HQNO on the NADH and succinate oxidation (Fig. 8A) gives support to this conclusion. The NADH oxidation is half maximally inhibited at an HQNO concentration of 1.1 μM, the succinate oxidation at 2.5 μM HQNO. When this experiment is plotted as degree of inhibition versus degree of saturation of the binding site (Fig. 8B), the experimental points fit to theoretical curves with a value k_2/k_1 of 13 for NADH oxidation and of 40 for succinate oxidation. These values are derived from the slope of the double-reciprocal plot of inhibition versus saturation (Fig. 8C). In agreement with this model the ratio of the overall rates of electron transfer for NADH and succinate equals the ratio of the value (k_2/k_1+1) for succinate and NADH, respectively. In ref. 21 it is shown that 50 % inhibition of NADH dehydrogenase with rotenone results in an HQNO-inhibition curve for which the k_2/k_1 is 30 while in the absence of rotenone a value of 15 was found.

As pointed out by Slater [9], the Wikström-Berden model [8] will result in identical curves, but then three k values are playing a role and one curve can be fitted with various sets of k values. In these inhibition curves there is no sign of any additional effect as is the case for the antimycin-inhibition curves [3, 28]. We may conclude, then, that HQNO behaves like an ideally simple inhibitor: inhibition of the HQNO-sensitive step is linear with the saturation of the binding site.

Extra reduction of cytochrome b

It has been proposed that the increased reduction of cytochrome *b* seen when antimycin is added to substrate-reduced particles in the presence of cyanide (the "extra reduction"), is due to a conformational state stabilized by antimycin [1–3]. Since, however, HQNO, which is not an allosteric inhibitor, also induces this increased reduction [17, 29], it must be concluded that allosteric behaviour as such is not essential for extra reduction, which gives support to a kinetic explanation of this phenomenon, such as that proposed by Wikström and Berden [8].

In the presence of succinate, cyanide and oxygen, HQNO causes an increased

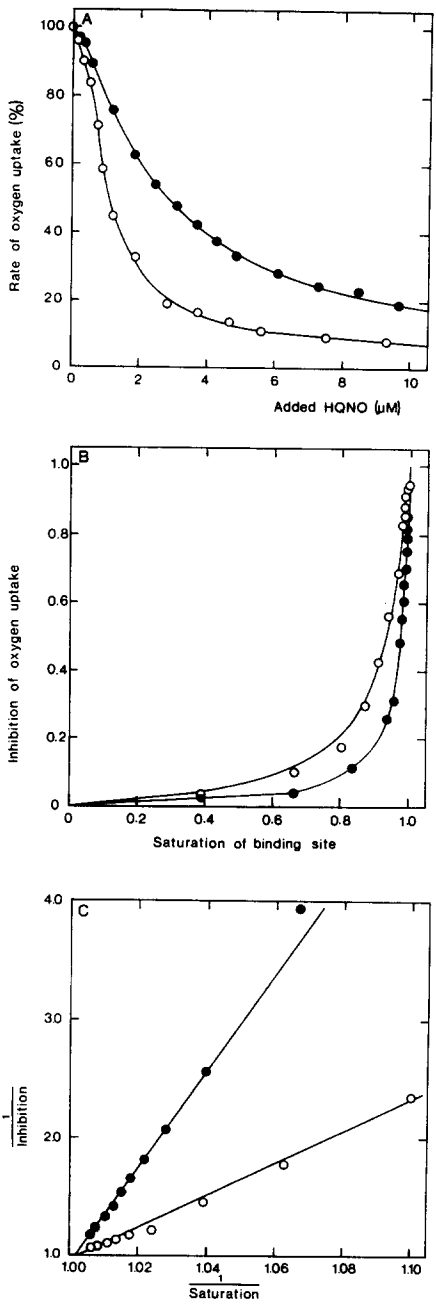

Fig. 8.

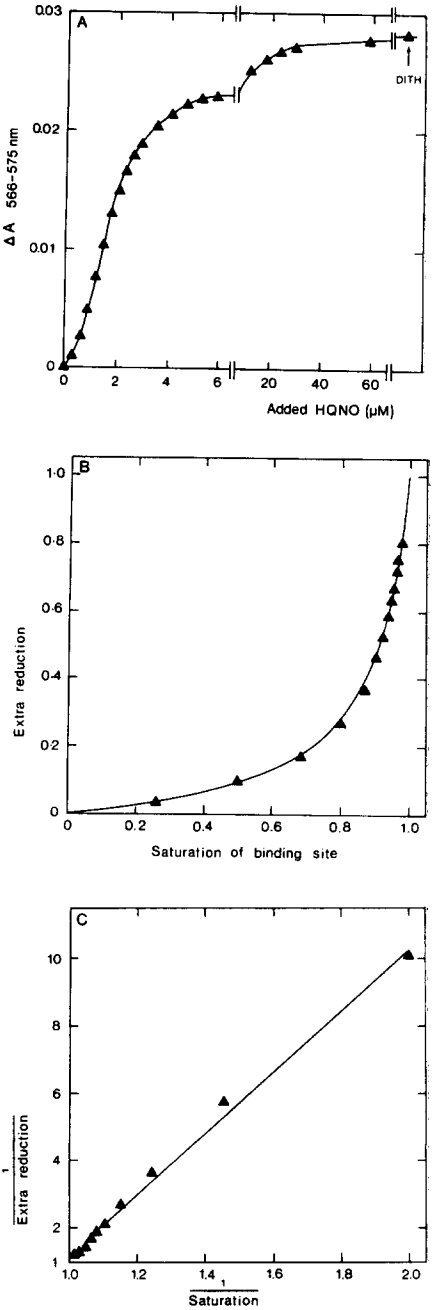

Fig. 9.

See opposite page for legends.

reduction of cytochrome *b*, presumably only *b*-566, but, unlike antimycin, without shifting the absorbance maximum of *b*-562 [17]. This means that all absorbance changes measured at 566–575 nm are true redox changes of cytochrome *b*-566. As shown in Fig. 9A the extra reduction (Δb^{2+}) as a function of the added HQNO is slightly sigmoidal, in accordance with Brandon et al. [17]. When the degree of extra reduction is plotted as function of the degree of saturation of the binding site (Fig. 9B) a true rectangular hyperbolic relation is obtained (at least between 10 and 90 % extra reduction), as can be seen from the straight line obtained in the double-reciprocal representation of this plot (Fig. 9C). Although in these experiments 2 mM cyanide is present, there is still residual electron transfer, as can be concluded from the role of oxygen or another oxidant in the extra-reduction phenomenon [8, 10, 11]. In the model of Wikström and Berden [8], under steady-state electron flow, the rate of electron transfer in the $QH_2 \rightarrow$ cyt. *c* pathway (specific rate k_2) equals the rate of electron transfer in the $QH\cdot \rightarrow$ cyt. *c* pathway (specific rate k_3). This means that the ratio $[QH\cdot]/[QH_2]$ equals k_2/k_3. Under the conditions used the electron transfer is very slow and cytochrome *b* will be in near equilibrium with the $QH\cdot/QH_2$ couple, i.e. $[b^{3+}]/[b^{2+}] = K\cdot[QH\cdot]/[QH_2] = K\cdot k_2/k_3$, and the ratio $[b^{3+}]/[b^{2+}]$ would be expected to decrease proportionally to the decrease of k_2, i.e. to saturation of the HQNO site. This means that when extra reduction is plotted against degree of saturation a hyperbola will be obtained (Fig. 9B, see Appendix B). A double-reciprocal plot (Fig. 9C) yields a straight line with slope $1+[b^{3+}]/[b^{2+}]$ in the absence of HQNO. The slope of the line in Fig. 9C is 9.0. Assuming that *b*-562 is nearly fully reduced in the absence of HQNO and that the increased reduction only involves cytochrome

Fig. 8. Inhibition of NADH and succinate oxidase in sub-mitochondrial particles by HQNO. Oxygen uptake in the presence of various amounts of NQNO was measured as described in Experimental, with EDTA particles (1.2 mg/ml). A. Rate of oxygen uptake as function of the concentration of added HQNO. For NADH oxidase (○ − ○) 100 % represents the uptake of 1538 natoms O per min per mg. The rate of HQNO-insensitive NADH oxidase was 2.4 %. For succinate oxidase (● − ●) 100 % represents the uptake of 512 natoms O per min per mg. The rate of HQNO-insensitive succinate oxidase was 4.9 %. B. Inhibition of HQNO-sensitive respiration as function of the saturation of the HQNO-binding site. The saturation of the binding site is calculated from the apparent K_D (70 nM) and the concentration of binding sites (0.44 μM), determined as in Fig. 3. The lines are theoretical curves according to the relation: $I = \bar{Y}/(k_2/k_1(1-\bar{Y})+1)$, where I is the degree of inhibition and $\bar{Y}$ the degree of saturation of the binding site. ○ − ○, NADH as substrate with $k_2/k_1 = 13$; ● − ●, succinate as substrate with $k_2/k_1 = 40$. C. Double-reciprocal representation of the experimental points of Fig. 8B. Only those points representing more than 25 % inhibition are used in this graph. The lines represent the relation: $I^{-1} = (k_2/k_1+1)\ \bar{Y}^{-1} - k_2/k_1$ (see Appendix B) and the slopes therefore equal (k_2/k_1+1). ○ − ○, NADH as substrate, the slope is 14; ● − ●, succinate as substrate, the slope is 41.

Fig. 9. HQNO-induced reduction of long-wavelength cytochrome *b* in sub-mitochondrial particles (extra reduction). A suspension of EDTA particles (3.05 mg/ml) was incubated with 2 mM KCN and 10 mM succinate. When the reduction level of cytochrome *b* was constant, successive amounts of HQNO were added and the increase in $\Delta A_{566-575\,nm}$ was measured. A. Increase in $\Delta A_{566-575\,nm}$ as a function of the concentration of added HQNO. B. Extent of extra reduction as a function of the saturation of the binding site (apparent $K_D = 91$ nM and $n = 1.0$ μM). The line is a theoretical curve according to the relation: "extra reduction" $= \bar{Y}/(C(1-\bar{Y})+1)$ (see Appendix B) with $C = 8.0$. C. Double-reciprocal representation of the experimental points of Fig. 9B. Only those points representing more than 10 % extra reduction are used in this graph. The line represents the relation: ("extra reduction")$^{-1} = (C+1)\bar{Y}^{-1} - C$ (see Appendix B) and the slope therefore equals $(C+1)$. The slope of the line is 9.0.

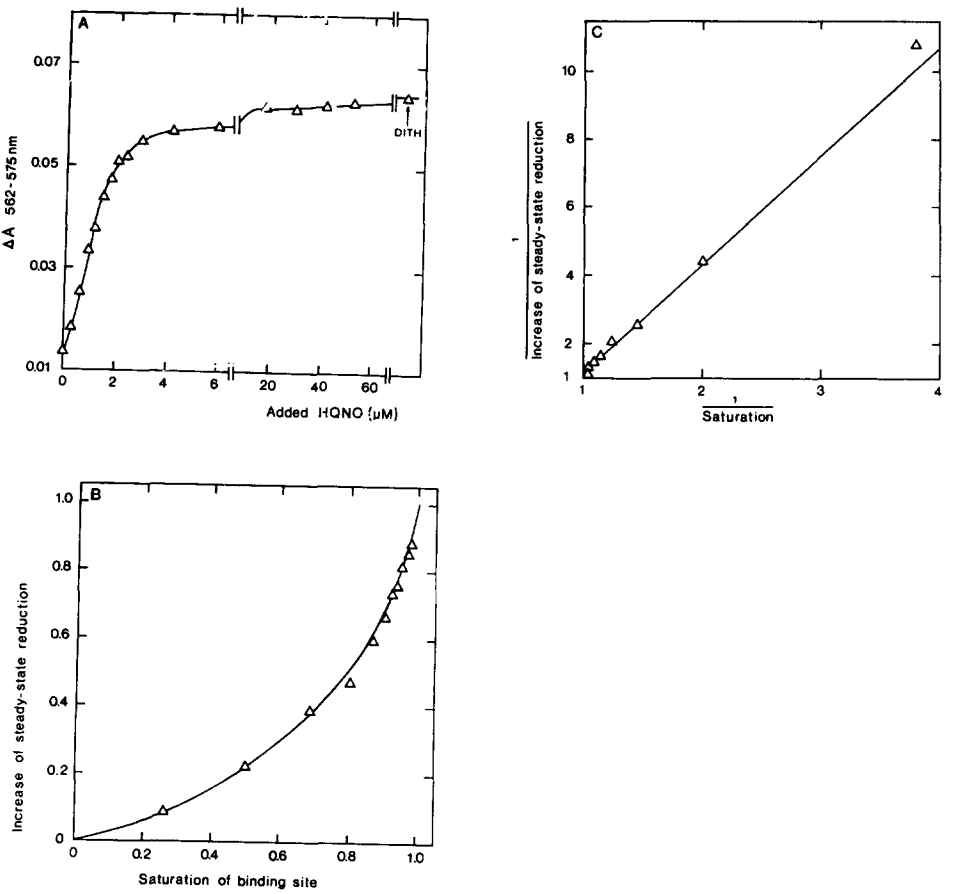

Fig. 10. HQNO-induced reduction of cytochrome *b* in sub-mitochondrial particles under steady-state succinate oxidation condition. Suspensions of EDTA particles (3.06 mg/ml) were incubated with increasing amounts of HQNO. After 5 min 10 mM succinate were added. When the steady-state reduction level of cytochrome *b* was constant $\Delta A_{562-575\,nm}$ was measured against a reference not containing HQNO or succinate. A. $\Delta A_{562-575\,nm}$ as a function of the concentration of added HQNO. B. The increase in the steady-state reduction level of cytochrome *b* as a function of the saturation of the binding site (apparent $K_D = 91$ nM and $n = 1.0\,\mu$M). The line is a theoretical curve according to the relation: "increased reduction" $= \bar{Y}/(C \cdot (1-\bar{Y})+1)$ (see Appendix B) with $C = 2.4$. C. Double-reciprocal representation of the experimental points of Fig. 10B. Only those points representing more than 9 % increase in the steady-state reduction level are used in this graph. The line represents the relation: ("increased reduction")$^{-1} = (C+1)\bar{Y}^{-1} - C$ (see Appendix B) and the slope therefore equals $(C+1)$. The slope of the line is 3.4.

b-566, it can be calculated that *b*-566 was 11 % reduced in the absence of HQNO. Separate absorbance measurements at 562–575 nm (not shown) revealed that, in agreement with Wikström and Berden [8], 10–20 % of *b*-566 can be reduced by succinate in the presence of KCN, assuming that at 562–575 nm 65 % of the absorbance difference dithionite minus oxidized is due to *b*-562 [19, 30].

Steady-state reduction level of cytochrome b

A hyperbolic relationship is also obtained between the degree of the increased reduction obtained on adding HQNO in the absence of cyanide (Fig. 10A) and the degree of saturation of the binding site (Fig. 10 B and C). However, the interpretation is hampered by the fact that both cytochrome *b* species, differing in mid-point potential and spectral contributions, are now involved. Moreover, it is questionable whether the *b* cytochromes under these conditions are in redox equilibrium with the QH · / QH_2 couple. However, it would be expected that these two effects would work in opposite directions. For example, at low HQNO concentrations the reduction of cytochrome *b* will be less than found at equilibrium, but because a wavelength is used where the high-potential component (the first to be reduced) contributes more than the other, a higher reduction level is calculated than in fact is present.

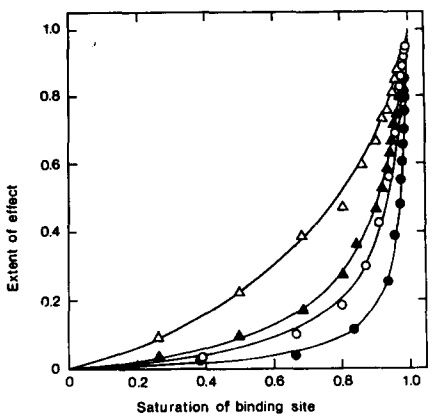

Fig. 11. Comparison of the measured HQNO-effect curves. ● — ●, inhibition of succinate oxidase activity (from Fig. 8B); ○ — ○, inhibition of NADH oxidase activity (from Fig. 8B); ▲ — ▲, extent of extra reduction (from Fig. 9B); △ — △, increase in the steady-state reduction level of cytochrome *b* (from Fig. 10B).

In Fig. 11 the different effects of HQNO measured are compared. From this graph it is clear that even with a simple respiratory inhibitor like HQNO, the titrations of the different effects, although all related to the binding of HQNO to the same specific site, can show considerable divergency.

DISCUSSION

HQNO and antimycin show similar fluorescent characteristics. In both cases the fluorescence is enhanced on binding to albumin and quenched on binding to submitochondrial particles. Energy transfer from antimycin to the heme of cytochrome *b* has been proposed as the mechanism for the quenching when it is bound to particles [3]. However, this cannot be the mechanism of quenching of HQNO since the emission band of HQNO (480 nm) is too far removed from the Soret band of either ferri- or ferrocytochrome *b* (420 and 429 nm, respectively). Further investigations on the mechanism of quenching may possibly yield more information about the nature of the binding site for antimycin and HQNO.

From our data it is clear why HQNO is reported to be a 10- to 40-fold less effective inhibitor of electron transfer than antimycin [16–18, 30, 31]. First, the dissociation constant (64 nM) of the specific site responsible for inhibition is 2000 times higher than that for antimycin. Secondly, a considerable amount of HQNO can be bound aspecifically to non-inhibitory sites, thereby increasing the K_I. Thirdly, there is a considerable over-capacity of the HQNO-sensitive step compared to the overall electron-transfer velocity. From the first two points it is clear that the efficiency of HQNO inhibition expressed as μmol added per g protein needed for half-maximal inhibition will depend on the protein concentration, and the amount of aspecific binding may even vary with the kind of preparation used. As our binding studies revealed, it is of general importance to realise that when a dissociation constant is derived from a titration that follows a spectral effect of a ligand upon binding, this dissociation constant will be over-estimated when aspecific binding takes place.

In a recent paper, Eisenbach and Gutman [32], in order to account for a difference in reduction kinetics of cytochrome *b* by succinate in the presence of antimycin and HQNO, propose that the inhibition sites are not identical. However, our binding data, particularly the equal amounts of binding sites and the exclusion of HQNO from its binding site by antimycin (Fig. 3A), strongly indicate that the binding sites are identical and that inhibition occurs by binding to these sites. There are, however, some important differences between antimycin and HQNO: under succinate-reduced circumstances antimycin binding is positively cooperative, revealing the allosteric nature of this inhibitor [3], whereas this effect is absent with HQNO. This may well be related to its 2000-times lower affinity for the binding site compared with antimycin. We propose, therefore, that the antimycin-stabilized conformational change influences both the inhibition curves and the reduction kinetics of cytochrome *b*, these effects being superimposed on the characteristics revealed by HQNO.

Probably the most important result of these studies with HQNO is that the changes in the redox state of cytochrome *b*, both under steady-state succinate oxidation as under extra-reduction conditions, show a considerable divergency from the inhibition of overall electron transfer. It seems to us that the whole phenomenon of extra reduction, and in particular its response to the saturation of the binding site with HQNO, are difficult to explain within any kinetic model based on a linear electron-transfer chain, including that of Kröger and Klingenberg [4]. We therefore believe that the redox level of cytochrome *b* reflects the properties of a branched electron-transfer pathway through Complex III such as that proposed by Wikström and Berden [8]. The ratio $[b^{3+}]/[b^{2+}]$, shown to decrease linearly with the saturation of the HQNO-binding site, would, on this basis, reflect the relative specific rates of the $QH_2 \rightarrow$ cyt. *c* and $QH\cdot \rightarrow$ cyt. *c* pathways (apart from deviations from the equilibrium between ubiquinone and cytochrome *b*). Since the relative specific rates of these pathways are not dependent on the rate of the overall electron transfer, reduction of cytochrome *b* and inhibition of electron transfer are separate phenomena.

The antimycin-effect curves reported by Grimmelikhuijzen et al. [28, 33, 34] for their mutant 28 of *Candida utilis* are very similar to the HQNO-effect curves for beef-heart mitochondrial particles. The discrepancies between the effects of antimycin on the electron transfer and on cytochrome *b* reduction in the mutant may be explained in the same way as that given for HQNO in this paper. In wild-type yeast and in beef-heart mitochondria this discrepancy is not clearly visible with antimycin

because of the allosteric effects and the very high binding constant of antimycin. The titre for the full effect on both phenomena is therefore identical. When the binding is less strong and thereby allosteric effects become less prominent the inhibition seems to have a much higher titre than the effect on cytochrome *b* because the former effect needs a much higher saturation of the binding site, depending only on the Q-reduction and Q-oxidation capacities.

APPENDIX A

The protein dependence of the K_D^{app}

If the fluorescence of a ligand changes upon binding to a protein and the binding is homogeneous (i.e. every ligand molecule is bound with the same affinity and with the same change in fluorescence) the concentrations of free (f) and bound (b) ligand are given by Eqns. 1 and 2

$$f = \frac{F - \alpha_b \cdot t}{\alpha_f - \alpha_b} \tag{1}$$

$$b = \frac{F - \alpha_f \cdot t}{\alpha_b - \alpha_f} \tag{2}$$

where F is the measured fluorescence, and α_b and α_f the fluorescence coefficients of bound and free ligand, respectively, and t is the total ligand concentration. α_b and α_f can be derived from fluorescence titration curves according to Eqns. 3 and 4

$$\alpha_b = \left(\frac{dF}{dt}\right)_{\substack{t \to 0 \\ n \to \infty}} \tag{3}$$

$$\alpha_f = \left(\frac{dF}{dt}\right)_{t \to \infty} \tag{4}$$

where n is the concentration of binding sites. The fluorescence-titration data can be analysed according to the Scatchard equation [26].

$$\frac{b}{f} = \frac{n - b}{K_D} \tag{5}$$

where K_D is the dissociation constant of the ligand-protein complex.

These equations cannot be generally applied in the case of non-homogeneous binding of the ligand. If, however, a ligand is firmly bound to a specific binding site and weakly bound to a relatively high concentration of non-specific binding sites, the Scatchard plot will yield an apparent K_D (K_D^{app}) that is dependent on the protein concentration. In this case

$$t = b_s + b_{as} + f \tag{6}$$

and thus

$$F = \alpha_s b_s + \alpha_{as} b_{as} + \alpha_f \cdot f \tag{7}$$

where b_s and b_{as} are the concentrations of ligand bound to specific and aspecific sites, respectively, and α_s and α_{as} are the fluorescence coefficients of the ligand bound to these sites. From the Scatchard equation for the specific sites

$$b_s/f = \frac{n_s - b_s}{K_D^s} \quad \text{it follows that } b_s = \frac{n_s \cdot f}{K_D^s + f} \tag{8}$$

where n_s is the concentration of specific binding sites and $K_D{}^s$ the dissociation constant of the specific-site-ligand complex. From the Scatchard equation for the aspecific sites

$$b_{as}/f = \frac{n_{as} - b_{as}}{K_D^{as}} = \frac{n_{as}}{K_D^{as}} \; (b_{as} \ll n_{as}) \quad \text{it follows that } b_{as} = \frac{n_{as}}{K_D^{as}} \cdot f \tag{9}$$

where n_{as} is the concentration of aspecific binding sites and $K_D{}^{as}$ the dissociation constant of the aspecific-site-ligand complex. Making use of $(dF/dt) = (dF/df)/(dt/df)$ it follows from Eqns. 6–9 that

$$\left(\frac{dF}{dt}\right) = \left\{\alpha_s \frac{n_s K_D^s}{(K_D^s + f)^2} + \alpha_{as} \frac{n_{as}}{K_D^{as}} + \alpha_f\right\} \cdot \left\{\frac{n_s K_D^s}{(K_D^s + f)^2} + \frac{n_{as}}{K_D^{as}} + 1\right\}^{-1} \tag{10}$$

At low ligand concentration (i.e. $f \ll K_D{}^s$) and at high protein concentration (i.e. $n_s/K_D{}^s + n_{as}/K_D{}^{as} \gg 1$) it follows from Eqn. 10 that

$$\left(\frac{dF}{dt}\right)_{\substack{t \to 0 \\ n \to \infty}} = \left\{\alpha_s \frac{n_s}{K_D^s} + \alpha_{as} \frac{n_{as}}{K_D^{as}}\right\} \cdot \left\{\frac{n_s}{K_D^s} + \frac{n_{as}}{K_D^{as}}\right\}^{-1} \tag{11}$$

At high ligand concentration (i.e. $f \gg K_D{}^s$) it follows from Eqn. 10 that

$$\left(\frac{dF}{dt}\right)_{t \to \infty} = \left\{\alpha_{as} \frac{n_{as}}{K_D^{as}} + \alpha_f\right\} \cdot \left\{\frac{n_{as}}{K_D^{as}} + 1\right\}^{-1} \tag{12}$$

When Eqns. 11 and 12 are used instead of Eqns. 3 and 4 to calculate "apparently free" and "apparently bound" according to Eqns. 1 and 2, a straight Scatchard plot is only obtained when $(dF/dt)_{\substack{t \to 0 \\ n \to \infty}} = \alpha_s$. In this case it can be calculated that

$$\text{"apparently free"} \quad = \left(1 + \frac{n_{as}}{K_D^{as}}\right) f \tag{13}$$

$$\text{"apparently bound"} = b_s \tag{14}$$

and using Eqn. 5 that the "apparent K_D" will depend linearly on the protein concentration (as shown in Fig. 5), according to the relation:

$$K_D^{app} = \left(1 + \frac{n_{as}}{K_D^{as}}\right) K_D^{s} \tag{15}$$

In the particular case of the binding of HQNO to sub-mitochondrial particles the condition to obtain straight Scatchard plots

$$\left(\left(\frac{dF}{dt}\right)_{\substack{t\to 0\\ n\to\infty}} = \alpha_s\right) \text{ is fulfilled because } \left(\frac{dF}{dt}\right)_{\substack{t\to 0\\ n\to\infty}}$$

experimentally appeared to be zero. This is the case because the fluorescence of HQNO bound to the specific sites is fully quenched (i.e. $\alpha_s = 0$) and the term on the right-hand side of Eqn. 11 including α_{as} (i.e. $\{\alpha_{as}(n_{as}/K_D{}^{as})\} \cdot \{n_{as}/K_D{}^{as} + n_s/K_D{}^{s}\}^{-1}$) makes only a negligible contribution to the fluorescence because $n_s/K_D{}^{s} \gg n_{as}/K_D{}^{as}$. As can be derived from Fig. 5:

$$n_s/K_D^{s} = \frac{2320\text{ nM}}{64\text{ nM}} = 36.25 \gg n_{as}/K_D^{as} = b_{as}/f = 1.2.$$

APPENDIX B

The extra reduction of cytochrome b

Assuming the Wikström-Berden model [8], one can predict the reduction of cytochrome *b* as a function of the saturation of the HQNO-binding site. Under steady-state conditions the velocity of electron transfer from the QH · /QH_2 couple to cytochrome *c* (specific rate k_2) equals the velocity of electron transfer from the Q/QH · couple to cytochrome *c* (specific rate k_3),

i.e. $k_2[QH_2] = k_3[QH\cdot]$

or $[QH\cdot]/[QH_2] = k_2/k_3$.

If the QH · /QH_2 and b^{3+}/b^{2+} redox couples are in equilibrium

$$[b^{3+}]/[b^{2+}] = K \cdot [QH\cdot]/[QH_2] = K \cdot k_2/k_3 = C,$$

where K is an equilibrium constant and C is a function of k_2 and k_3.

Putting $b = [b^{2+}] + [b^{3+}]$, this may be written $(b - [b^{2+}])/[b^{2+}] = C$, from which it follows that

$$[b^{2+}] = \frac{b}{C+1} \quad \text{and} \quad b - [b^{2+}] = \frac{Cb}{C+1},$$

where $[b^{2+}]$ is the amount of cytochrome *b* reduced in the absence of HQNO, and $b - [b^{2+}]$ the amount that can be reduced by the addition of HQNO.

According to the Wikström-Berden model, HQNO lowers k_2 proportionally to the saturation of the HQNO-binding site. Representing the degree of saturation of this site by the symbol $\bar{Y}$,

$k_2{}^{i} = k_2\ (1-\overline{Y})$, and therefore

$C_i = C\ (1-\overline{Y})$, since $C = K/k_3 \cdot k_2$,

where $k_2{}^{i}$ and C_i represent the values of k_2 and C, respectively, in the presence of the inhibitor.

Thus, the concentration of b^{2+} in the presence of HQNO, $b_i{}^{2+}$, is given by

$$[b_i^{2+}] = \frac{b}{C_i+1} + \frac{b}{C(1-\overline{Y})+1}.$$

The "extra reduction" of cytochrome *b* brought about by HQNO is equal to

$$\frac{[b_i^{2+}] - [b^{2+}]}{b-[b^{2+}]} = \frac{\overline{Y}}{C(1-\overline{Y})+1},$$

which is the equation of the curve described in Fig. 9B. The double-reciprocal plot in Fig. 9C shows the relation

$$(\text{"extra-reduction"})^{-1} = (C+1)\ \overline{Y}^{-1} - C$$

which yields a straight line with a slope equal to

$$(C+1) = \left(\frac{[b^{3+}]}{[b^{2+}]} + 1\right).$$

ACKNOWLEDGEMENTS

The authors wish to thank Professor Dr. E. C. Slater for valuable discussions and continuous interest. This work was supported in part by grants from the Netherlands Organization for the Advancement of Pure Research (Z.W.O.) under the auspices of the Netherlands Foundation for Chemical Research (S.O.N.).

REFERENCES

1 Bryła, J., Kaniuga, Z. and Slater, E. C. (1969) Biochim. Biophys. Acta 189, 317–326
2 Bryła, J., Kaniuga, Z. and Slater, E. C. (1969) Biochim. Biophys. Acta 189, 327–336
3 Berden, J. A. and Slater, E. C. (1972) Biochim. Biophys. Acta 256, 199–215
4 Kröger, A. and Klingenberg, M. (1970) Vitamins Hormones 28, 533–574
5 Kröger, A. and Klingenberg, M. (1973) Eur. J. Biochem. 34, 358–368
6 Kröger, A. and Klingenberg, M. (1973) Eur. J. Biochem. 39, 313–323
7 Rieske, J. A. and Das Gupta, U. (1972) FEBS Lett. 20, 316–320
8 Wikström, M. K. F. and Berden, J. A. (1972) Biochim. Biophys. Acta 283, 403–420
9 Slater, E. C. (1973) Biochim. Biophys. Acta 301, 129–154
10 Rieske, J. S. (1971) Arch. Biochem. Biophys. 145, 179–193
11 Wilson, D. F., Koppelman, M., Erecinska, M. and Dutton, P. L. (1971) Biochem. Biophys. Res. Commun. 44, 759–766
12 Chance, B. (1972) FEBS Lett. 23, 3–20
13 Cornforth, J. W. and James, A. T. (1956) Biochem. J. 63, 124–130
14 Kaniuga, Z., Bryła, J. and Slater, E. C. (1969) in Inhibitors, Tools in Cell Research (Bücher, Th. and Sies, H., eds.), pp. 282–300, Springer Verlag, Heidelberg
15 Tappel, A. L. (1960) Biochem. Pharmacol., 3, 289–296
16 Lightbown, J. W. and Jackson, F. L. (1956) Biochem. J. 63, 130–137

17 Brandon, J. R., Brocklehurst, J. R. and Lee, C. P. (1972) Biochemistry 11, 1150–1154
18 Nijs, P. (1967) Biochim. Biophys. Acta 143, 454–461
19 Berden, J. A. (1972) Site II of the respiratory chain, Ph. D. thesis, University of Amsterdam, Gerja, Waarland
20 Van Ark, G. and Berden, J. A. (1975) Abstr. 5th Int. Biophys. Congr., p. 156, Villadsen and Christensen, Copenhagen
21 Berden, J. A. and Van Ark, G. (1976) in Mitochondrial Genetics, Biogenesis and Bioenergetics, De Gruyter and Co., Berlin, in the press
22 Fessenden, J. M. and Racker, E. (1966) J. Biol. Chem. 241, 2483–2489
23 Lee, C. P. and Ernster, L. (1968) Eur. J. Biochem. 3, 385–390
24 Strong, F. M., Dickie, J. P., Loomans, M. E., Van Tamelen, E. E. and Dewey, R. S. (1960) J. Am. Chem. Soc. 82, 1513–1514
25 Cleland, K. W. and Slater, E. C. (1953) Biochem. J. 53, 547–556
26 Scatchard, G. (1949) Ann. N.Y. Acad. Sci. 51, 660–672
27 Weder, H. G., Schildknecht, J., Lutz, R. A. and Kesselring, P. (1974) Eur. J. Biochem. 42, 475–481
28 Grimmelikhuijzen, C. J. P. and Slater, E. C. (1973) Biochim. Biophys. Acta 305, 67–79
29 Chance, B. (1958) J. Biol. Chem. 233, 1223–1229
30 Wilson, D. F. and Erecinska, M. (1975) Arch. Biochem. Biophys. 167, 116–128
31 Fynn, G. H. (1969) Biochim. Biophys. Acta 180, 244–252
32 Eisenbach, M. and Gutman, M. (1975) Eur. J. Biochem. 59, 223–230
33 Grimmelikhuijzen, C. J. P., Marres, C. A. M. and Slater, E. C. (1975) Biochim. Biophys. Acta 376, 533–548
34 Grimmelikhuijzen, C. J. P. (1975) The Mitochondrial Respiratory Chain, Ph. D. thesis, University of Amsterdam, Krips Repro, Meppel